

1N-33
15717
11P

Evaluation of Some Slow-Wave Vane Structures for a Miniature Traveling-Wave Tube at 30 GHz

Frank Kavanagh
Analex Corporation
Brook Park, Ohio

Ben Ebihara, Thomas M. Wallett,
and James A. Dayton, Jr.
Lewis Research Center
Cleveland, Ohio

June 1994

(NASA-TM-106654) EVALUATION OF
SOME SLOW-WAVE VANE STRUCTURES FOR
AMINIATURE TRAVELING-WAVE TUBE AT
30 GHz (NASA. Lewis Research
Center) 11 p

N94-36819

Unclass

G3/33 0015717



National Aeronautics and
Space Administration

EVALUATION OF SOME SLOW-WAVE VANE STRUCTURES FOR A MINIATURE TRAVELING-WAVE TUBE AT 30 GHZ

Frank Kavanagh
Analex Corporation
3001 Aerospace Parkway
Brook Park, Ohio 44142

Ben Ebihara, Thomas M. Walleth, and James A. Dayton, Jr.
National Aeronautics and Space Administration
Lewis Research Center
Cleveland, Ohio 44135

SUMMARY

The dispersion characteristics of six vane type slow wave structures were experimentally measured near 1 GHz to determine applicability in an electrostatically focused 30 GHz miniature traveling-wave tube (TWT). From the measured results, the trapezoidal vane structure appeared to be the most promising exhibiting an interaction impedance equal to 337.9 ohms with no roof and 375.46 ohms with a roof at $\beta L/\pi$ equal to 0.3.

A 30 GHz trapezoidal vane structure with coupling irises was fabricated using electrical discharge machining (EDM). This structure, however, was too lossy for a short electrostatically focused tube, but several of the structures are amenable to a tube with permanent magnetic focusing.

INTRODUCTION

At NASA Lewis Research Center (LeRC) there is an interest in a traveling-wave tube (TWT) of reduced size and weight capable of delivering several watts at 30 GHz for a phased array antenna [1]. This paper describes the experimental evolution and evaluation of the circuits considered for this tube.

The original concept envisioned a type of Millman circuit as the slow wave structure with the tube operating at 4 kV and under 10 mA as a forward wave amplifier having a gain of approximately 20 dB. The tube was to be short, employing an electrostatically focused beam and a depressed collector. Higher efficiency could be achieved by using a low power thermionic cathode or, possibly, a field emission cathode. The measured dispersion characteristics of a Millman structure are illustrated in figure 1 [2].

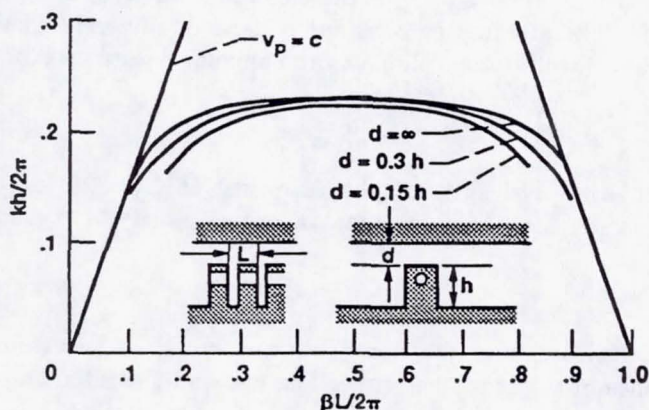


Figure 1 - Dispersion characteristics of the Millman structure. Vane thickness is $L/2$ for these data.

This circuit has a forward-wave fundamental mode of propagation, with the upper cutoff frequency of the pass band occurring approximately where the height of the resonators is $\lambda/4$, where λ is the wavelength. The low frequency cutoff of the pass band occurs at the normal ridged-wave guide cutoff frequency. The structure is usually capacitively loaded by positioning the top wall closer to the resonators to achieve the rounded characteristic as illustrated. Figure 2 [2] is a sketch of the rf electric fields in the Millman structure at the upper and lower cutoff frequencies of the lowest pass band.

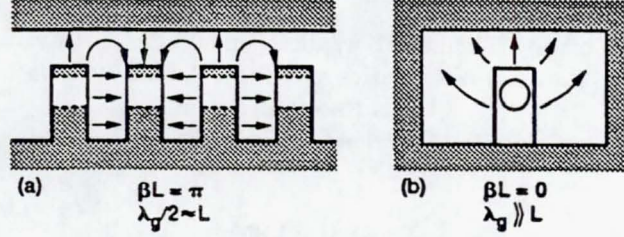


Figure 2 - A sketch of the RF electric fields in the Millman structure at the (a) upper and (b) lower cutoff frequencies of the lowest passband.

The electric fields are maximum at the top of the vane and decay as the cosine function to zero at the bottom. The strength of the axial fields at the beam position is a measure of the beam coupling or interaction impedances at their frequencies. The interaction impedance of a traveling-wave structure is defined by Pierce [3] as

$$Z_m = \frac{E_{zm}^2}{2\beta_m^2 P} \quad (1)$$

Here, E_{zm} is the m th space harmonic of the axial electric field at the beam position, P is the power flow along the structure, and β_m is the wave propagation constant or phase shift per unit length of the m th space harmonic. The wave propagation constant $\beta_m = \beta_0 + 2\pi m/L$ where β_0 is the phase shift per unit length of the fundamental wave and L is the period of the structure.

The power flow on the structure is related to the stored energy per unit length W' and group velocity v_g by $P = W' \cdot v_g$. Introducing this into equation (1) yields

$$Z_m = \frac{E_{zm}^2}{2\beta_m^2 W' v_g} \quad (2)$$

The group velocity v_g is very low near the cutoff frequencies and thus the stored energy per unit length W' is large for a given power P . The amplitude along the circuit varies as $\exp(-\alpha\lambda_e)$ where α is the attenuation constant and λ_e is the electronic wavelength equal to the phase velocity v_p divided by frequency f . The attenuation constant α depends inversely on the circuit quality factor Q and group velocity v_g but directly proportional to the angular frequency $\omega = 2\pi f$. It is given by

$$\alpha = \frac{\omega}{2Qv_g} \quad (3)$$

The loss L_λ in dB/wavelength can be expressed as $L_\lambda = 20 \log_{10}(\exp(\alpha\lambda_e))$. This can be equivalently expressed in terms of the quality factor, phase velocity, and group velocity as

$$L_\lambda = \frac{27.3}{Q} \cdot \frac{v_p}{v_g} \quad (4)$$

The factor Q can be calculated from the circuit dimensions [4]. An examination of equations (2) and (4) shows the importance of the group velocity. The loss and the interaction impedance vary inversely on its value.

Figure 4 shows the cold test apparatus and a trapezoidal vane structure, while figure 5 is a diagram of the trapezoidal circuit with dimensions at 1.4 GHz and 30 GHz.

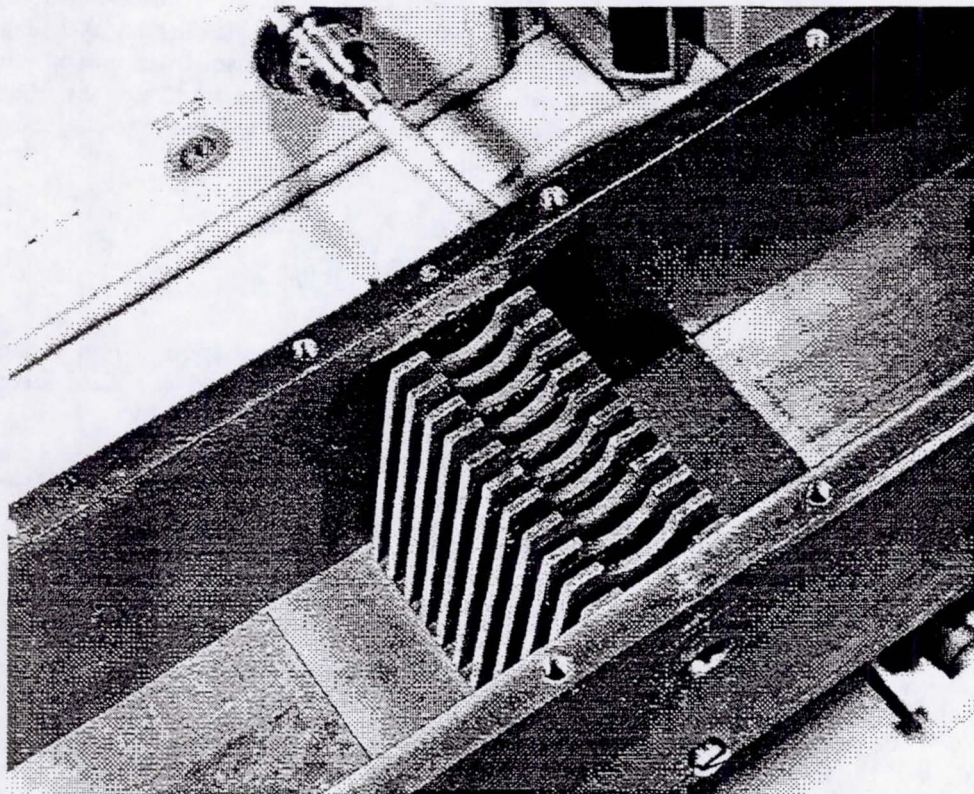


Figure 4 - Trapezoidal vane structure in cold test fixture.

1.4 GHz	30 GHz
$a = 0.753 \text{ cm}$	0.03 cm
$h = 5.715 \text{ cm}$	0.234 cm
$L = 0.572 \text{ cm}$	0.0234 cm
$w = 5.715 \text{ cm}$	0.234 cm
$\delta = 0.381 \text{ cm}$	0.015 cm

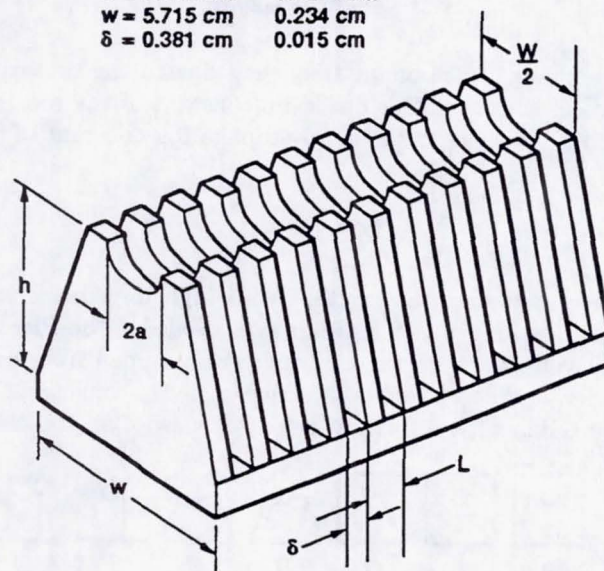


Figure 5 - Dimensions of trapezoidal structure.

A common technique to measure the propagation characteristics and interaction impedance is to use shorting planes at points of mirror symmetry along the circuit. A resonant cavity is formed consisting of N periods of the circuit. The propagation characteristics are determined by a simple transmission measurement to determine the resonant frequencies thus yielding an ω - β diagram. The interaction impedance can then be inferred by making a similar transmission measurement with a dielectric rod placed at the proposed beam position. The relative changes in resonant frequencies due to the perturbing effect of the rod is a measure of the interaction impedance. The interaction impedance for the m th space harmonic may be written as

$$Z_m = \left(\frac{1}{2\beta_m^2 v_g} \right) \cdot \left(\frac{E_{zm}^2}{E^2} \right) \cdot \left(\frac{E^2}{W'} \right) \quad (5)$$

where E represents the total electric field. The first factor in equation (5) is found from the experimental ω - β diagram, the second factor from a Fourier analysis, and the third factor from the circuit perturbation measurement. The axial space-harmonic fields are defined by

$$E_z = \sum_m E_{zm} e^{-j\beta_m z} \quad (6)$$

and it is convenient to relate the axial space-harmonic field amplitudes E_{zm} to the total axial field amplitude E_z by the expression $E_{zm} = E_z \cdot M_m$ where M_m is a space-harmonic amplitude factor which may be determined for any specific circuit [5].

If a rod is placed along the axis of a cylindrical structure or at the plane of symmetry of a planar structure and the propagating mode is a longitudinal mode, the transverse electric fields can be neglected. While this may not be true in all the vane structures studied it gives a very good approximation of the impedances involved. The frequency perturbation equation is

$$\frac{\delta\omega}{\omega} = \frac{-(\epsilon_r - 1)\epsilon_0\pi^2}{4W'} E_z^2 \sum_m M_m^2 \quad (7)$$

and equation (5), the space-harmonic interaction impedance, may be written in terms of analytically determined and experimentally measured quantities:

$$Z_m = \frac{1}{2\beta_m^2 v_g} \frac{M_m^2}{\sum_m M_m^2} \frac{-4(\delta\omega/\omega)}{(\epsilon_r - 1)\epsilon_0\pi b^2} \quad (8)$$

where $\delta\omega/\omega$ is the relative change in resonant frequency due to the perturbing dielectric rod, b is the radius of the dielectric rod, ϵ_r is the relative dielectric constant of the rod (alumina $\epsilon_r = 9.3$), ϵ_0 is the free space permittivity, and $\beta_m = \omega/v_p$ is the axial propagation constant of the m th harmonic wave.

1 GHZ SCALED TESTS

Since a short tube was desired, a structure with high impedance and low loss per unit length operating at about 0.3π or 0.4π on the ω - β diagram was needed. The Pierce impedance Z_m , the phase velocity v_p , and the group velocity v_g of the circuits were obtained from cold test measurements. All the measurements except for loss can be made at a lower, more convenient frequency, in this case, 1.4 GHz and then scaled to 30 GHz. Figure 3 shows a frontal view of all the tested circuits at 1.4 GHz.

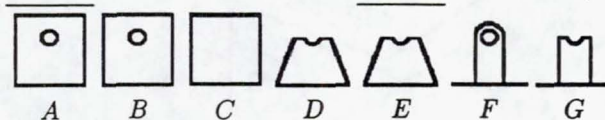


Figure 3 - A frontal view of tested circuits.

Figure 6 shows the ω - β diagram for the tested circuits.

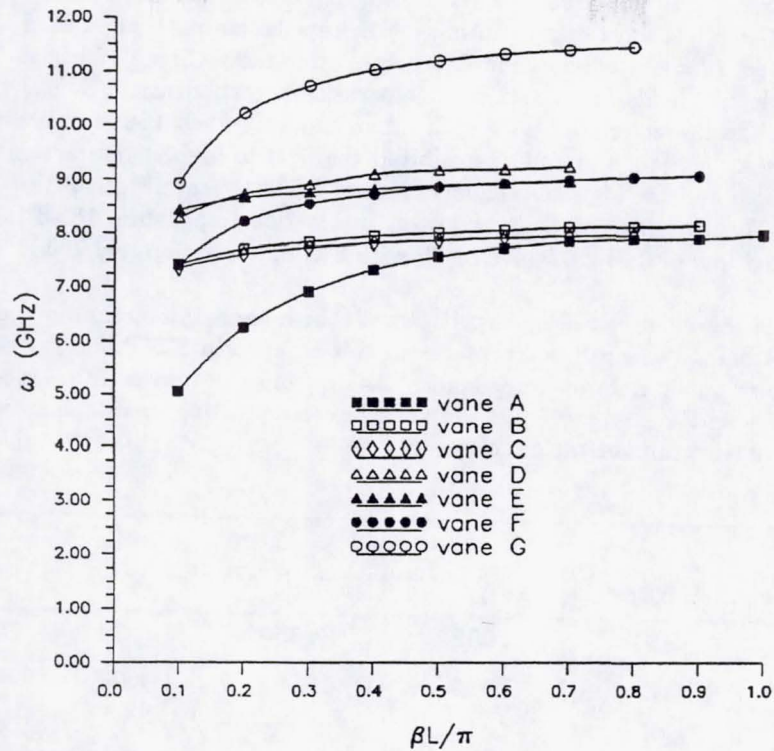


Figure 6 - ω - β diagram of circuits.

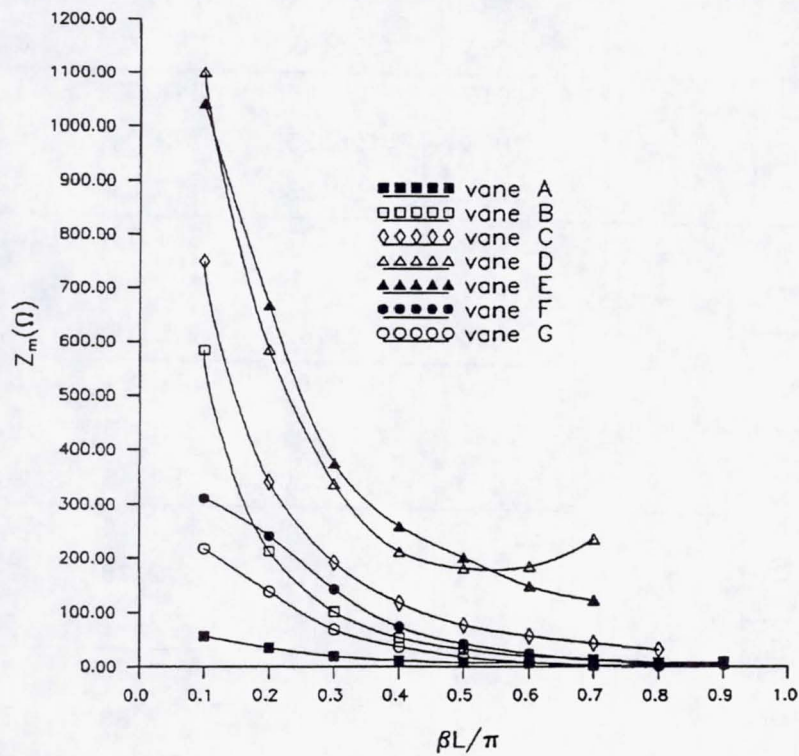
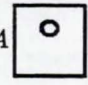
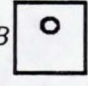
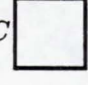
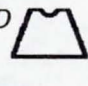
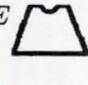
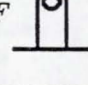
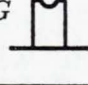


Figure 7 - Interaction Impedance of circuits.

In figure 7 are the impedance characteristics that were generated from the cold tests. These characteristics show, in general, an increasing value of interaction impedance Z for circuit A through circuit E. This trend was not true of circuit F which had lower impedances and a problem with thermal rigidity. Circuit A gave disappointingly low impedances until one raised the roof to the point where it had no effect ($d = \infty$) where upon it becomes circuit B. Circuit C has the beam on top of the circuit where the electric fields are a maximum but decaying exponentially above the circuit. Circuits D and E have similar characteristics with each other and very good Pierce impedances; however, they have very high losses. Although circuit D exhibited the next to highest interaction impedance, 337.9 Ω at $\beta L/\pi = 0.3$, it also had the highest calculated loss of 0.83 dB/wavelength with a Q of approximately 450. On the other hand, circuit A had the lowest interaction impedance, 18.96 Ω at $\beta L/\pi = 0.3$, and the lowest calculated loss of 0.01 dB/wavelength with a Q of approximately 700.

Therein lies the dilemma. The circuit D with the highest interaction impedance has a loss that is too high (0.2 dB per wavelength is acceptable in this case) for a TWT and the circuit A which has a low loss has too low an interaction impedance. Aside from the lowest impedance, circuit A had the lowest v_p/v_g , losses, and V_e , where V_e is the voltage corresponding to the phase velocity v_p . Table 1 lists the important test results of the circuits.

Circuit	$\beta L/\pi$	v_g/c	v_p/v_g	$Z_m(\Omega)$	$V_e(\text{kV})$
A 	.2	.052	3.655	34.34	9.437
	.3	.030	4.581	18.96	5.059
	.4	.019	5.757	11.09	3.169
B 	.2	.012	19.248	212.90	14.510
	.3	.007	21.599	101.45	6.561
	.4	.005	24.688	52.77	3.754
C 	.2	.010	22.156	341.03	14.159
	.3	.006	25.853	192.09	6.366
	.4	.004	29.230	117.34	3.628
D 	.2	.018	14.370	584.71	18.811
	.3	.011	17.108	337.90	8.556
	.4	.006	21.422	212.17	4.909
E 	.2	.009	30.502	666.84	18.550
	.3	.005	34.548	375.46	8.207
	.4	.004	36.309	259.45	4.644
F 	.2	.029	8.595	241.14	16.604
	.3	.015	11.721	142.70	7.806
	.4	.009	14.898	72.57	4.544
G 	.2	.045	6.825	137.98	26.434
	.3	.022	9.662	67.83	12.494
	.4	.013	12.680	36.30	7.295

Since the gain parameter C in a TWT is given by $C^3 = \frac{ZI}{4V}$, circuit A would have to be 2.6 times as long as circuit D for the same gain if tubes made of these circuits both had the same ratio of voltage to current and the same low loss. A tube this long would not be amenable to electrostatic focusing and permanent magnets would have to be used which would increase the size and weight.

30 GHZ FABRICATION TECHNIQUE

A one inch length of circuit D was built as shown in figure 8 for 30 GHz operation.

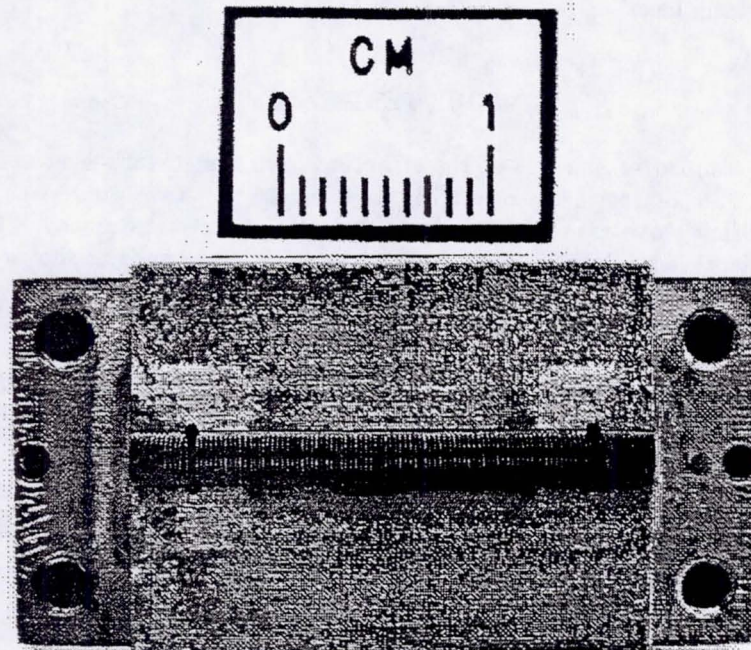


Figure 8 - 30 GHz trapezoidal structure with resonant iris couplings.

Attempts to fabricate the 30 GHz trapezoidal structure by means of conventional machining techniques were ineffectual due to its small size and configuration as well as the need to hold the critical dimensions and to obtain excellent surface finishes. Satisfying such stringent requirements were beyond the capabilities of the most precise turning-type machine tools. A more promising method turned out to be the computer numerically controlled (CNC) wire-cut electrical discharge machining (EDM). An oil-flushed EDM was first used. After fabrication, however, there were traces of carbon deposits that remained on the surfaces which increased circuit losses. A change was then made to use a water-flushed unit. The Sodick model A280, a closed-cycle water system that is filtered, de-ionized, and chilled, was used for the final fabrication. Some of the important parameters that can be adjusted to alter the precision and quality of the surface are power which controls the effects of localized heating, capacitance, on-off pulse ratio, cutting rate, wire tension, flushing-rate, number of passes, and materials. The best results were obtained when low power and low cutting rate were used. Since this entailed a long running time of about six hours, it was essential that environmental temperature remain constant and that there was sufficient wire length for uninterrupted operation during the entire period. Using low power reduced the heating effects thereby minimizing warping and oxidation, and imparting a smoother finish. In addition, a tighter wire tension helped to give greater precision.

The structure was made from a dispersion-hardened copper manufactured by SCM Corporation called "Glid-cop AL-20". The material had 90% of the electrical conductivity of oxygen free high conductivity (OFHC) copper. It did not anneal due to the EDM process. A 0.006 inch diameter molybdenum wire was used for its machining. A single pass was made for cutting each slot at a cutting rate of about 1 mm/min. The calculated periodic spacing of the vanes from measurements was 0.00947 inch and the average thickness was 0.0035 inch. There were 108 vanes machined in the structure of which 86 were between the two iris openings. Both of the irises were also machined using EDM techniques. The maximum pitch variation of the vanes was $\pm 7\%$ of their true positions and the vane thicknesses varied up to 14% of the average value. However, in both cases, at least 75% of the vanes were held within half the above percentages. The dimensions were measured using an optical comparator. Reading errors may have been introduced when the edges of the vanes were visually aligned to the measuring location.

30 GHZ TEST RESULTS

The rf was coupled in and out of the structure from underneath by resonant irises across the wave guide ports. The loss of the resonant iris itself across the wave guide was measured at 0.2 dB with a voltage standing wave ratio (VSWR) of 1.046 at the center frequency. The circuit combined with the resonant iris gave a minimum VSWR of 1.5 and 1.3 at the ends as shown in figure 9.

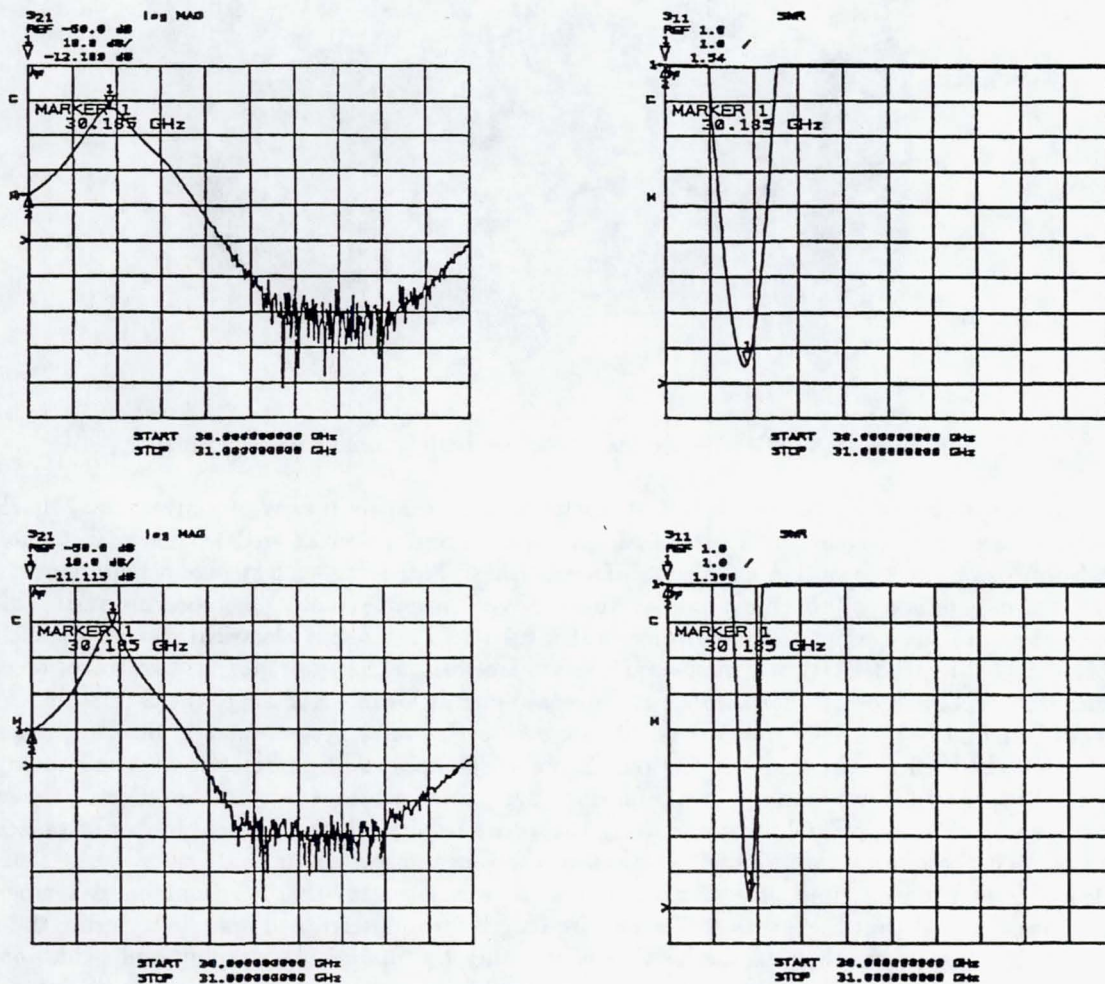


Figure 9 - VSWR and loss measurements of the trapezoidal circuit.

These values were obtained using tuning stubs in the wave guide side of the iris. The calculated loss of the section was 8.3 dB. Figure 9 shows the loss in one direction as 12.19 dB and in the other, 11.11 dB. The additional loss is due to coupling plus resistive losses.

DISCUSSION

A true value of the circuit losses can only be determined by measuring a second circuit of a different length to negate the effect of coupling losses. The circuit loss can be at most a few dB/inch in order to successfully operate a short, high impedance, electrostatically focused traveling-wave tube.

Circuit *D* exhibited the highest interaction impedance for the circuits tested. However, the loss for this type of structure is too great to allow the successful operation of this circuit in a traveling-wave tube. Since the loss per wavelength depends inversely on the Q of the circuit, efforts to increase the Q would result in a lower loss per wavelength. This, however, would be at the expense of a lower interaction impedance. Somewhere a tradeoff between interaction impedance and loss must be made. From the measured results, circuit *D* does not meet the requirements for use in a miniature TWT.

By incorporating periodic permanent magnets to provide better focusing of the electron beam it would be possible to increase the beam current significantly. This would have the effect of increasing the Pierce parameter C which not only would increase the gain of the TWT but also decrease the loss parameter d for the circuit. To what extent depends on the amount of focusing and beam perveance needed for the TWT to achieve the desired gain. Mechanical limitations would also dictate whether such a gain is achievable.

In spite of the limited preciseness of the EDM equipment used for this program, more experimentation could be done to fine tune or optimize all the adjustable parameters available on the machine so that greater accuracies and better surface finishes can be obtained. For example, excessive coolant flow directed toward the work would have a tendency to disturb the position of the wire which will reduce its cutting accuracy but insufficient coolant flow may change the spark erosive-cutting characteristic that would affect the surface quality. In addition, more work could be done with chemical polishing techniques to improve the finish.

Another area which could be improved is the inspection and measurement of small dimensions where a more accurate and less subjective method is sorely needed. Although the desired precision and surface finishes were not achieved by using the EDM process for structure fabrication, this emerging technology appears to be very promising and continual refinements occurring in EDM technology may result in the availability of a higher quality circuit in the future.

REFERENCES

1. J. A. Dayton, Jr. and H. G. Kosmahl, *Proceedings of the International Electron Devices Meeting 1986*.
2. D. C. Forster, "High power millimeter wave sources," *Advances in microwaves*, vol. 3, pp. 314-316, Academic Press, New York, NY, 1968.
3. J. R. Pierce, *Traveling-Wave Tubes*, p. 95, D. Van Nostrand Co., Princeton NJ.
4. Unpublished material, H. G. Kosmahl.
5. Curtis C. Johnson, *Field and Wave Electrodynamics*, pp. 268-269, McGraw-Hill Book Company, New York, NY, 1965.

REPORT DOCUMENTATION PAGE			Form Approved OMB No. 0704-0188	
Public reporting burden for this collection of information is estimated to average 1 hour per response, including the time for reviewing instructions, searching existing data sources, gathering and maintaining the data needed, and completing and reviewing the collection of information. Send comments regarding this burden estimate or any other aspect of this collection of information, including suggestions for reducing this burden, to Washington Headquarters Services, Directorate for Information Operations and Reports, 1215 Jefferson Davis Highway, Suite 1204, Arlington, VA 22202-4302, and to the Office of Management and Budget, Paperwork Reduction Project (0704-0188), Washington, DC 20503.				
1. AGENCY USE ONLY (Leave blank)		2. REPORT DATE June 1994		3. REPORT TYPE AND DATES COVERED Technical Memorandum
4. TITLE AND SUBTITLE Evaluation of Some Slow-Wave Vane Structures for a Miniature Traveling-Wave Tube at 30 GHz			5. FUNDING NUMBERS WU-235-01-1C	
6. AUTHOR(S) Frank Kavanagh, Ben Ebihara, Thomas M. Walleit, and James A. Dayton, Jr.				
7. PERFORMING ORGANIZATION NAME(S) AND ADDRESS(ES) National Aeronautics and Space Administration Lewis Research Center Cleveland, Ohio 44135-3191			8. PERFORMING ORGANIZATION REPORT NUMBER E-8967	
9. SPONSORING/MONITORING AGENCY NAME(S) AND ADDRESS(ES) National Aeronautics and Space Administration Washington, D.C. 20546-0001			10. SPONSORING/MONITORING AGENCY REPORT NUMBER NASA TM-106654	
11. SUPPLEMENTARY NOTES Frank Kavanagh, Analex Corporation, 3001 Aerospace Parkway, Brook Park, Ohio 44142 (work funded by NASA Contract NAS3-25776); Ben Ebihara, Thomas M. Walleit, and James A. Dayton, Jr., NASA Lewis Research Center. Responsible person, Thomas M. Walleit, organization code 5620, (216) 433-3673.				
12a. DISTRIBUTION/AVAILABILITY STATEMENT Unclassified - Unlimited Subject Category 33			12b. DISTRIBUTION CODE	
13. ABSTRACT (Maximum 200 words) The dispersion characteristics of six vane type slow wave structures were experimentally measured near 1 GHz to determine applicability in an electrostatically focused 30 GHz miniature traveling wave tube (TWT). From the measured results, the trapezoidal vane structure appeared to be the most promising exhibiting an interaction impedance equal to 337.9 ohms at $\beta L/\pi$ equal to 0.3. A 30 GHz trapezoidal vane structure with coupling irises was fabricated using electrical discharge machining (EDM). This structure, however, was too lossy for a short electrostatically focused tube, but several of the structures are amenable to a tube with permanent magnetic focusing.				
14. SUBJECT TERMS Vane structures; Interaction impedance; Dispersion characteristics			15. NUMBER OF PAGES 11	
			16. PRICE CODE A03	
17. SECURITY CLASSIFICATION OF REPORT Unclassified	18. SECURITY CLASSIFICATION OF THIS PAGE Unclassified	19. SECURITY CLASSIFICATION OF ABSTRACT Unclassified	20. LIMITATION OF ABSTRACT	